AD-A086 110 ARMY ARMAMENT RESEARCH AND DEVELOPMENT COMMAND WATER--ETC F/G 20/11
STRESS ANALYSES OF OD NOTCHED THICK-WALLED CYLINDERS SUBJECTED --ETC(U)
FEB 80 J A KAPP

UNCLASSIFIED ARLCB-TR-80005 SBIE-AD-E440 069 NL

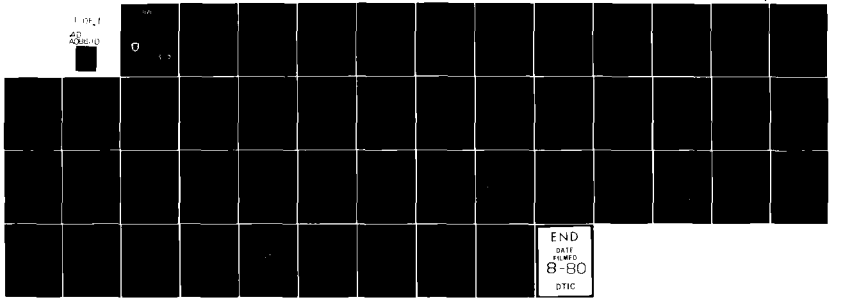

AD-E 440 069

LEVEL II

AD

ADA086110

TECHNICAL REPORT ARLCB-TR-80005

# STRESS ANALYSIS OF OD NOTCHED THICK-WALLED CYLINDERS SUBJECTED TO INTERNAL PRESSURE OR THERMAL LOADS

J.A. KAPP

FEBRUARY 1980

US ARMY ARMAMENT RESEARCH AND DEVELOPMENT COMMAND
LARGE CALIBER WEAPON SYSTEMS LABORATORY
BENET WEAPONS LABORATORY
WATERVLIET, N. Y. 12189

AMCMS No.611102H420011
DA Project No.1L161102AH42
PRON No. 1A02171A1A

DTIC ELECTE JUL 2 1980 S D B

APPROVED FOR PUBLIC RELEASE; DISTRIBUTION UNLIMITED

DDC FILE COPY.

80 6 10 009

## DISCLAIMER

The findings in this report are not to be construed as an official Department of the Army position unless so designated by other authorized documents.

The use of trade name(s) and/or manufacturer(s) does not constitute an official indorsement or approval.

## DISPOSITION

Destroy this report when it is no longer needed. Do not return it to the originator.

SECURITY CLASSIFICATION OF THIS PAGE (When Data Entered)

| REPORT DOCUMENTATION PAGE | | READ INSTRUCTIONS BEFORE COMPLETING FORM |
|---|---|---|
| 1. REPORT NUMBER<br>ARLCB-TR-80017 | 2. GOVT ACCESSION NO.<br>AD-A086 110 | 3. RECIPIENT'S CATALOG NUMBER |
| 4. TITLE (and Subtitle)<br>Stress Analysis of O.D. Notched Thick-Walled Cylinders Subjected to Internal Pressure or Thermal Loads | | 5. TYPE OF REPORT & PERIOD COVERED<br><br>6. PERFORMING ORG. REPORT NUMBER |
| 7. AUTHOR(s)<br>J. A. Kapp and G. A. Pfleg1 | | 8. CONTRACT OR GRANT NUMBER(s) |
| 9. PERFORMING ORGANIZATION NAME AND ADDRESS<br>Benet Weapons Laboratory<br>Watervliet Arsenal, Watervliet, N.Y. 12189<br>DRDAR-LCB-TL | | 10. PROGRAM ELEMENT, PROJECT, TASK AREA & WORK UNIT NUMBERS<br>AMCMS No. 6110211420011<br>DA Project 1L161102AH43<br>PRON No. 1A21Y141A1A |
| 11. CONTROLLING OFFICE NAME AND ADDRESS<br>US Army Armament Research and Development Command<br>Large Caliber Weapon Systems Laboratory<br>Dover, New Jersey 07801 | | 12. REPORT DATE<br>February 1980<br>13. NUMBER OF PAGES<br>44 |
| 14. MONITORING AGENCY NAME & ADDRESS(if different from Controlling Office) | | 15. SECURITY CLASS. (of this report)<br>UNCLASSIFIED<br>15a. DECLASSIFICATION/DOWNGRADING SCHEDULE |

16. DISTRIBUTION STATEMENT (of this Report)

Approved for public release; distribution unlimited.

17. DISTRIBUTION STATEMENT (of the abstract entered in Block 20, if different from Report)

18. SUPPLEMENTARY NOTES

To be presented at the Pressure Vessel Conference ASME, San Francisco, August 1980

19. KEY WORDS (Continue on reverse side if necessary and identify by block number)

Autofrettage
Finite Elements
NASTRAN
Thermal Stress
Stress Concentration Factor

20. ABSTRACT (Continue on reverse side if necessary and identify by block number)

Finite element stress analysis has been performed to determine the effects of two OD notch configurations in a cylinder subjected to internal pressure, or containing autofrettage residual stress. The effects on the residual stresses were determined by simulating these stresses with active temperature loads. The results show that the deeper of the two notch configurations is far more severe resulting in a maximum stress concentration factor of 2.9. The shallower notch has a maximum stress concentration factor of 3.0.

DD FORM 1 JAN 73 1473 EDITION OF 1 NOV 65 IS OBSOLETE

SECURITY CLASSIFICATION OF THIS PAGE (When Data Entered)

20. ABSTRACT (Cont'd)

An additional result is that by introducing notches in autofrettaged cylinders a significant amount of the residual stresses are relieved which indicates that smaller applied pressures can be contained by these cylinders, than in smooth cylinders before yielding occurs. The results also show that the possibility of OD initiated fatigue failure is greatly increased.

25 June 1980

ERRATA SHEET
(Change Notice)

C1 TO: TECHNICAL REPORT ARLCB-TR-80005

STRESS ANALYSIS OF OD NOTCHED THICK-WALLED CYLINDERS SUBJECTED TO INTERNAL PRESSURE OR THERMAL LOADS

by

J. A. Kapp

The following changes should be made in the above subject publication:

1. Add the name of G. A. Pflegl as co-author to front cover.

2. Remove the Report Documentation Page, DD Form 1473, from the above subject publication dated February 1980, and insert new Report Documentation Page inclosed.

3. Page 17 - Paste over the equations shown on this page with new equations on gum-backed paper inclosed.

4. Page 20 - Table I. Paste over Table I shown on this page with new Table I on gum-backed paper inclosed.

US ARMY ARMAMENT RESEARCH AND DEVELOPMENT COMMAND

LARGE CALIBER WEAPON SYSTEMS LABORATORY

BENET WEAPONS LABORATORY

WATERVLIET, N. Y. 12189

TABLE OF CONTENTS



TABLE



LIST OF ILLUSTRATIONS

ACKNOWLEDGMENTS

The author wishes to thank Dr. M. A. Hussain for his guidance in the use of autofrettage residual stress simulation techniques and to Mr. G. Pflegl for his assistance in generating the finite element solutions.

SYMBOLS

| | |
|---|---|
| a | Inside radius of a cylinder. |
| b | Outside radius of a cylinder. |
| d | Notch depth. |
| E | Modulus of Elasticity. |
| ESP | Elastic strength pressure, the pressure required to cause yielding in an autofrettaged cylinder. |
| h | Notch height. |
| ID | Inside diameter. |
| $K_{notch}$ | Stress concentration factor calculated by considering the entire notch as a stress riser. |
| $K_{root}$ | Stress concentration factor calculated by considering the roots of the notch as a stress riser. |
| OD | Outside diameter. |
| r | Radial coordinate. |
| R | Root radius of a notch. |
| $R_f$ | Stress reduction factor. |
| T | Temperature. |
| $T_a$ | Value of temperature at the inside radius a. |
| $T_\rho$ | Value of temperature at the elastic-plastic radius $\rho$. |
| W | Wall thickness of a cylinder (b-a). |
| $\alpha$ | Coefficient of thermal expansion. |
| $\varepsilon_z$ | Strain in the axial direction. |
| $\theta$ | Polar coordinate. |
| $\nu$ | Poisson's ratio. |

| | |
|---|---|
| $\rho$ | The elastic-plastic radius. |
| $\sigma_0$ | Yield strength. |
| $\sigma_1$ | Maximum principal stress. |
| $\sigma_3$ | Minimum principal stress. |
| $\sigma_{rA}$ | Autofrettage residual stress in the radial direction. |
| $\sigma_{rp}$ | Radial stress resulting from internal pressure. |
| $\sigma_{rT}$ | Radial stress resulting from an axisymmetric temperature distribution. |
| $\sigma_{zT}$ | Axial stress resulting from an axisymmetric temperature distribution. |
| $\sigma_{\theta A}$ | Autofrettage residual stress in the hoop direction. |
| $\sigma_{\theta A relieved}$ | Reduced value of the hoop residual stress due to the presence of a notch. |
| $\sigma_{\theta p}$ | Hoop stress resulting from internal pressure. |
| $\sigma_{\theta p total}$ | Hoop stress on the radial plane intersecting the center of a notch including bending, resulting from internal pressure. |
| $\sigma_{\theta T}$ | Hoop stress resulting from an axisymmetric temperature distribution. |
| $p$ | Internal pressure. |
| $\sigma_{max}$ | Maximum stress occurring in a fatigue cycle. |
| $\sigma_{min}$ | Minimum stress occurring in a fatigue cycle. |

## INTRODUCTION

To enable a thick-walled cylinder to contain greater pressures without plastic deformation, residual stresses are often induced in such cylinders through autofrettage.[1] The autofrettage residual stresses result from subjecting the cylinder to a pressure sufficient to cause plastic flow, axisymmetrically to some radius $\rho$, the elastic-plastic radius. Due to non-uniform recovery, upon removal of the autofrettage pressure a residual stress distribution results in the tangential direction which is compression at the ID and logarithmically varying to tension through that part of the wall which was plastically deformed. Outside the elastic-plastic radius, the tangential residual stresses follow an elastic stress distribution.[2] Two theoretical autofrettage residual stress distributions are shown in Fig. 1. Residual stresses also result in the radial and longitudinal directions, but these stresses are of lesser engineering significance and will not be considered here. The compressive tangential residual stress allows greater internal pressure to be contained elastically and greatly enhances the fatigue life of smooth cylinders when the fatigue failure initiates at the ID.[3]

---

[1] Davidson, T. E., and Kendall, D. P., "The Design of High Pressure Containers and Associated Equipment," The Mechanical Behavior of Materials Under Pressure, Pugh, H.L.I.D., Elsevier Publishing, Amsterdam, 1970.

[2] Davidson, T. E., Barton, C. S., Reiner, A. N., and Kendall, D. P., "Overstrain of High-Strength Open-End Cylinders of Intermediate Diameter Ratio," Proceedings of the First International Congress on Experimental Mechanics, Pergamon Press, Oxford, 1963.

[3] Davidson, T. E., Eisenstadt, R., and Reiner, A. N., Journal of Basic Engineering, December 1963, pp. 555-565.

In some applications of thick walled cylinders, such as modern large caliber cannon, it is sometimes necessary to introduce structural discontinuities, notches and keyways for example, to the OD of the cylinder. Autofrettaged cylinders with OD notches have lower fatigue lives than smooth cylinders, since the fatigue failure initiates at the OD. Such failures are more catastrophic than ID failures because very high stress intensity factors result from the tensile residual stresses[4] and tensile operating stresses,[5] allowing only very small critical crack sizes. Also it is unknown what the effect of removing material to introduce the notch on the OD will have on the residual stress distributions. This paper presents the results of stress analysis of a cylinder containing two OD notch configurations under internal pressure loading, and also under thermal loading which simulates the tangential autofrettage residual stresses exactly.

## THEORETICAL RESIDUAL STRESS DISTRIBUTIONS

The theoretical stress distribution of autofrettage has been reported by several investigators.[2,6] Based on the von Mises yield criterion and assuming plane strain conditions, i.e., $\varepsilon_z = 0$, the residual stresses in the tangential, and radial directions are given as:

---

[2]Davidson, T. E., Barton, C. S., Reiner, A. N., and Kendall, D. P., "Overstrain of High-Strength Open-End Cylinders of Intermediate Diameter Ratio," Proceedings of the First International Congress on Experimental Mechanics, Pergamon Press, Oxford, 1963.

[4]Kapp, J. A., Unpublished results.

[5]Kapp, J. A., and Eisenstadt, R., Fracture Mechanics, ASTM STP 677, C. W. Smith, Ed., American Society for Testing and Materials, 1979, pp. 746-756.

[6]Harvey, J. F., Theory and Design of Modern Pressure Vessels, 2nd Ed., Van Nostrand Reinhold, NY, 1974, pp. 61-67.

$$\sigma_{\theta A} = \begin{cases} \dfrac{2\sigma_0}{\sqrt{3}} \dfrac{a^2}{b^2-a^2}\left[1+\dfrac{b^2}{r^2}\right]\left[\dfrac{\rho^2-b^2}{2b^2}-\ell n\dfrac{\rho}{a}\right]+\left[\dfrac{\rho^2+b^2}{2b^2}-\ell n\dfrac{\rho}{r}\right] & a \le r \le \rho \\ \dfrac{2\sigma_0}{\sqrt{3}}\left[1+\dfrac{b^2}{r^2}\right]\left\{\dfrac{\rho^2}{2b^2}+\dfrac{a^2}{b^2-a^2}\left[\dfrac{\rho^2-b^2}{2b^2}-\ell n\dfrac{\rho}{a}\right]\right. & \rho \le r \le b \end{cases} \quad (1)$$

$$\sigma_{rA} = \begin{cases} \dfrac{2\sigma_0}{\sqrt{3}}\left[\dfrac{a^2}{b^2-a^2}\right]\left[1-\dfrac{b^2}{r^2}\right]\left[\dfrac{\rho^2-b^2}{2b^2}-\ell n\dfrac{\rho}{a}\right]+\left[\dfrac{\rho^2-b^2}{2b^2}-\ell n\dfrac{\rho}{r}\right] & a \le r \le \rho \\ \dfrac{2\sigma_0}{\sqrt{3}}\left[1-\dfrac{b^2}{r^2}\right]\dfrac{\rho^2}{2b^2}+\dfrac{a^2}{b^2-a^2}\left[\dfrac{\rho^2-b^2}{2b^2}-\ell n\dfrac{\rho}{a}\right] & \rho \le r \le b \end{cases} \quad (2)$$

Good agreement between the theoretical stress distributions, Equations (1) and (2) and measured residual stress distributions has been observed by Davidson et al,[7] although closer agreement is obtained when the residual stresses are calculated using the Tresca yield criterion. The only difference between Equations (1) and (2) and the stress distributions determined by using the Tresca criterion is that the constant coefficient $2\sigma_0/\sqrt{3}$ is replaced by $\sigma_0$. Since the schemes used to simulate the autofrettage stress distributions, discussed below, are all developed based on the assumption that the von-Mises criterion applies, the same assumption will be made here. The results are presented in such a manner that they reflect a relative change between stresses actually acting in the cylinder and those predicted using

[7] Davidson, T. E., Kendall, D. P., and Reiner, A. N., "Residual Stresses in Thick-Walled Cylinders Resulting From Mechanically Induced Overstrain," Experimental Mechanics, 1963, Vol. 3, pp. 253-262.

Equations (1) and (2). The relative, percentage deviation can be equally well applied to theoretical stresses calculated using either the Tresca or von Mises criteria.

The effect of introducing structural discontinuities to smooth cylinders on autofrettage residual stresses has not been investigated. Some experiments have been conducted by Kendall[8] to measure changes in residual stress when the cylinder is uniformly reduced in wall thickness by machining. The results of these experiments show that large changes in residual stresses can be accomplished with even small amounts of material removal.

## SIMULATION OF RESIDUAL STRESSES

Since residual stresses exist in autofrettaged cylinders under the application of no active external loads, it is necessary to develop a method for simulating these stresses using some loading condition in a smooth cylinder. Once the simulation loads are determined, these same loads can then be applied to a non-smooth cylinder; thus the effect of the structural discontinuity is obtained. The method of 'equivalent cuts', used by Hussain and Pu[9] is one such simulation technique. Using this method, a fine radial saw cut is made in the cylinder, effectively making the cylinder a singly-connected ring. By applying certain enforced displacements to the surfaces created by the saw cut, a state of stress developed in the ring exists that

---

[8]Kendall, D. P., "The Effect of Material Removal on the Strength of Autofrettaged Cylinders," Watervliet Arsenal Technical Report AD701049, Watervliet, NY, January 1970.

[9]Hussain, M. A. and Pu, S. L., "Preliminary Study of the Effect of a Recoil Keyway on the Fatigue Life of the M185 Cannon Tubes," Technical Report ARLCB-TR-78017, Watervliet Arsenal, Watervliet, NY, November 1978.

is equivalent to the autofrettage case. Although excellent results are obtained using this technique, its application to the OD notch problem is costly since for each different residual stress pattern studied, a different enforced displacement is applied. This requires the generation of a different stiffness matrix for each loading condition when the finite element method of analysis is employed.

Another method of simulating the residual stresses, also proposed by Hussain et al[10] is by the application of thermal loads. This is the method used in this report and will be discussed briefly. For a smooth hollow cylinder subjected to an axisymmetric temperature distribution T(r), the three principal stresses, assuming zero resultant longitudinal force at the ends is given by:[11]

$$\sigma_{rT} = \frac{\alpha E}{(1-\nu)r^2}\left[\frac{r^2-a^2}{b^2-a^2}\int_a^b rT(r)dr - \int_a^r rT(r)dr\right] \tag{3}$$

$$\sigma_{\theta T} = \frac{\alpha E}{(1-\nu)r^2}\left[\frac{r^2+a^2}{b^2-a^2}\int_r^b rT(r)dr + \int_a^r rT(r)dr - r^2T(r)\right] \tag{4}$$

$$\sigma_{zT} = \frac{\alpha E}{(1-\nu)r^2}\left[\frac{2}{b^2-a^2}\int_a^b rT(r)dr - T(r)\right] \tag{5}$$

[10] Hussain, M. A., Pu, S. L., Vasilakis, J. D., and O'Hara, P., "Simulation of Partial Autofrettage by Thermal Loads," Submitted to Journal of Pressure Vessels Technology.

[11] Timoshenko, S. P. and Goodier, J. N., Theory of Elasticity, 3rd Edition, McGraw-Hill, 1970, p. 448.

The temperature distribution necessary for the simulation is expressed in general terms as

$$T(r) = \begin{cases} T_\rho + \dfrac{(T_a - T_\rho)}{\ell n(\rho/a)} \ell n(\rho/r) & a \le r \le \rho \\ T_\rho & \rho \le r \le b \end{cases} \tag{6}$$

where $T_a$ and $T_\rho$ are temperature values at the inside radius and the elastic-plastic radius respectively. Since thermal stresses result from a temperature gradient, the absolute values of $T_a$ and $T_\rho$ are not important, thus for convenience one of these values can be arbitrarily assigned, in this case $T_\rho = 0$. Upon integration of equations (3) and (4) using equation (6) with $T_\rho = 0$, the thermal stresses are obtained as:

$$\sigma_{\theta T} = \begin{cases} \dfrac{\alpha E}{(1-\nu)} \dfrac{T_a}{2\ell n(\rho/a)} \dfrac{a^2}{b^2-a^2}\left[1 + \dfrac{b^2}{r^2}\right]\left[\dfrac{\rho^2-b^2}{2b^2} - \ell n(\rho/a)\right] + \left[\dfrac{\rho^2+b^2}{2b^2} - \ell n(\rho/r)\right] & a \le r \le \rho \\ \dfrac{\alpha E}{(1-\nu)} \dfrac{T_a}{2\ell n(\rho/a)} \left[1 - \dfrac{b^2}{r^2}\right]\left[\dfrac{\rho^2}{2b^2} + \dfrac{a^2}{b^2-a^2} \dfrac{\rho^2-b^2}{2b^2} - \ell n(\rho/a)\right] & \rho \le r \le b \end{cases} \tag{7}$$

$$\sigma_{rT} = \begin{cases} \dfrac{\alpha E}{(1-\nu)} \dfrac{T_a}{2\ell n(\rho/a)} \dfrac{a^2}{b^2-a^2}\left[1 - \dfrac{b^2}{r^2}\right]\left[\dfrac{\rho^2-b^2}{2b^2} - \ell n(\rho/a)\right] + \left[\dfrac{\rho^2-b^2}{2b^2} - \ell n(\rho/a)\right] & a \le r \le \rho \\ \dfrac{\alpha E}{(1-\nu)} \dfrac{T_a}{2\ell n(\rho/a)} \left[1 - \dfrac{b^2}{r^2}\right]\left[\dfrac{\rho^2}{2b^2} + \dfrac{a^2}{b^2-a^2} \dfrac{\rho^2-b^2}{2b^2} - \ell n(\rho/a)\right] & \rho \le r \le b \end{cases} \tag{8}$$

The similarity between equations (1) and (2) and equations (7) and (8) is readily seen. Equivalent stress states will result when:

$$\frac{2\sigma_0}{\sqrt{3}} = \frac{\alpha E}{(1-\nu)} \frac{T_a}{2\ell n(\rho/a)} \tag{9}$$

Those temperature distributions which result in the same stress state shown in Fig. 1 are plotted in Fig. 2.

More important than the mathematical exactness of the temperature loading simulational is the physical mechanism which causes these stresses. In each instance the stress distributions result from non-uniform expansion or contraction of an axisymmetric section of the cylinder. The stresses occur then as a result of the finite stiffness of the structure. When the stiffness of the structure is changed by introducing notches, cracks or other structural discontinuities, the resulting change in autofrettage residual stresses should be exactly the same as that change in the thermal stresses when temperature distribution given by equations (6) and (9) is applied to a cylinder containing those same structural discontinuities. Also, by applying the temperature loads, only a single finite element mesh, with a single stiffness matrix is necessary to analyze all of the loading conditions studied.

## THE OD NOTCH PROBLEM

The engineering applications of concern in this paper is an OD notch in a thick-walled cylinder as shown in Fig. 3. The cylinder has a radius ratio b/a of 1.74 with two different notch depth to wall thickness ratios d/W of .178 and .088. The root radius and notch height are the same in each case,

namely R/W of .013 and h/W of .444 respectively. Two autofrettage conditions were analyzed 100% overstrain and 60% overstrain*, for each notch configuration. Also, internal pressure was applied to each cylinder.

The analysis was conducted using the finite element method and the NASTRAN program. The elements used are constant strain triangular and rectangular membranes, which can be loaded mechanically for internal pressure and with temperature for the autofrettage simulation. Since the notch cylinder is symmetric about the center of the notch, only one half of the cylinder is necessary for the analysis. One of the meshes used is shown in Fig. 4.

## RESULTS

The finite element results are plotted in Figs. 5 through 16. Three reference planes, A-A, B-B, and C-C, as indicated in Fig. 3 are used to present the results. Plane A-A is the plane located 180° removed from the center of the notch; stresses acting on this plane indicate the far removed effect of the notch. The B-B and C-C reference planes in the vicinity of the notch are used since the notches analyzed can be considered as a dual stress concentration. First, the entire notch can be considered as a stress concentrator, and the stresses acting on plane B-B can be used as a measure of the severity of this stress concentration, $K_{notch}$. Second, the root radius R can be considered as a separate stress riser. Plane C-C is the radial plane

*Percent overstrain is defined as that percentage of the wall thickness which is subjected to plastic deformation under the application of the autofrettage pressure.

which passes through the root radius of the notch. The stresses which act on this plane will enable the calculation of a stress concentration factor for the root of the notch, $K_{root}$.

The meshes used, Fig. 4, were constructed such that the centroids of elements along the reference planes lie on the radial planes, as closely as possible. There is some deviation from this and some of the element centroids lie on a radial planes a small distance from the reference planes, which results in the scatter observed in the outer portions of the cylinder in some of the finite element solutions. Also, the output from the NASTRAN program is reported in the elemental coordinate systems which do not always correspond to the global coordinates $(r,\theta)$. To circumvent this, the maximum principal stress is determined for each element and this stress is plotted in the figures. In no instance is the direction of the maximum principal stress more than three degrees different from the hoop direction. The hoop stresses are the only results presented since these are the stresses which dominate the onset of elastic breakdown, or crack initiation which are the engineering application of this work.

Pressure Loading

The stresses resulting from internal pressure loading of thick-walled cylinders are the well known Lame solution given as:

$$\sigma_{rP} = \frac{pa^2}{b^2-a^2}\left[1 - \frac{b^2}{r^2}\right] \tag{10}$$

$$\sigma_{ap} = \frac{pa^2}{b^2-a^2}\left[1 + \frac{b^2}{r^2}\right] \qquad (11)$$

The finite element results for the pressure loading are shown in Figs. 5 through 8. For the deep notch case (Figs. 5 and 6), expected results are obtained. Along A-A, the stresses follow equation (11) but along C-C significant deviation from theory is observed. The stress concentration factor, $K_{root}$, is calculated as the ratio of the finite element determined stress acting on C-C at the root radius to the finite element determined stress at the same radial position as the root radius acting on A-A. The stress concentration factors for all loading conditions are summarized in Table I.

The stresses occurring on B-B are plotted in Fig. 6. A first approximation to predicting these stresses would be to assume that they follow the Lame solution, with reduced wall thickness, by replacing b with (b-d) in equation (11). Another approximation proposed by Kapp[12] can be made by realizing that rotational equilibrium is not maintained when the reduced wall thickness approximation is applied. Thus, in addition to the reduced wall thickness Lame stress there must be a bending component. The total stress distribution is:

$$\sigma_{\theta P total} = pa^2\left\{\frac{\left(1 + \frac{(b-d)^2}{r^2}\right)}{(b-d)^2 - a^2} + \frac{12\left(r - \frac{(b-d+a)}{2}\right)}{(b-d-a)^3}\left[\frac{b^2}{b^2-a^2}\ln\left(\frac{b}{a}\right) - \frac{(b-d)^2}{(b-d)^2 - a^2}\ln\left(\frac{b-d}{a}\right)\right]\right\} \qquad (12)$$

[12] Kapp, J. A., "The Effect of Autofrettage on Fatigue Crack Propagation in Externally Flawed Thick-Walled Disks," Masters Thesis, Union College, Schenectady, NY, 1976.

Both of these approximations are compared with the finite element results in Fig. 5 which shows that neither gives a good representation of the actual stresses through the wall thickness, although a reasonable estimate of the maximum stress at the center of the notch can be made using Equation (12). The stress concentration factor $K_{notch}$ is calculated as the ratio of the maximum finite element stress at the outer portion of plane B-B to the stress predicted by Equation (11) using the reduced wall thickness approximation, at the same radial position. For the shallow notch, the stress concentration factor $K_{root}$ is significantly reduced as shown in Fig. 6 and Table I for pressure loading. The stresses acting along B-B also indicate a less severe stress state. The results in Fig. 8 show that a very good approximation to the maximum occurring stress near the center of the notch can be made using Equation (12), and the value of $K_{notch}$ is also reduced.

Autofrettage Results

The results of the temperature loading simulation of the 100% overstrain and 60% overstrain cases are plotted in Fig. 9 through 16. For deep notches, the 100% overstrain case is presented in Figs. 9 and 10. The stresses along A-A and C-C for 100% overstrain show that the roots of the notch are a significant stress concentration with $K_{root}$ approximately the same as determined in the internal pressure case. An interesting difference in the response of the notched cylinder under temperature loading is that the stresses along A-A are significantly different than the theoretical autofrettage stresses in a smooth cylinder. This seemingly defies the St. Vennant Principle. These stresses result from a non-uniform enforced displacement of portions of the

cylinder and are a function of the stiffness of the cylinder. When the notch is introduced in the cylinder its stiffness is reduced allowing it to accept the enforced displacement while generating lower stresses throughout the entire less stiff, more compliant structure, thus the St. Venant Principle need not apply. For the deep notch geometry, 100° overstrain case, there a close agreement between theoretical autofrettage stresses assuming the reduced wall thickness approximation along plane B-B case is shown in Fig. 10. There is some increase in the tensile stress at outside portion due to the stress concentration, $K_{notch}$ but this affect is more confined than in the pressure case.

The shallow notch, 100% overstrain solutions are given in Figs. 11 and 12. Again, the far removed stresses on plane A-A are reduced from the theoretical full thickness solution. The amount by which these stress distributions differ is approximately the same as in the deep notch case. The stress concentration factor, $K_{root}$, is also reduced substantially over the deep notch case. There is also close agreement between the finite element stress distributions on planes A-A and C-C in the inner portions of the wall thickness, another indication of a significantly less severe stress state. Figure 12 shows the close agreement between the reduced wall thickness assumption and the actually occurring stress distribution along B-B, with virtually no stress concentration, $K_{notch}$.

The results of the final loading condition tested, 60% overstrain, are plotted in Figs. 13 through 16. The effect of the deep notch on this loading condition is the smallest of all of the cases studied. Figure 13 shows

that the A-A stresses are again less than theoretical full wall thickness stress distribution, but the agreement between the finite element stresses on plane C-C and plane A-A is very good throughout most of plastically deformed inner portion of the wall thickness. On plane B-B for deep notches, Fig. 14 shows small differences between the reduced wall thickness theoretical prediction in the plastic regions, but relatively large deviation in the elastic region, with $K_{notch}$ approximately the same as calculated for the 100% overstrain, deep notch case.

Shallow notches have an even smaller effect on the residual stress patterns for the 60% overstrain case as shown in Figs. 15 and 16. The far field stresses are less than the theoretical full wall thickness solution but the A-A stresses and C-C stresses agree very well throughout the thickness. The only significant deviation in the two finite element distributions is in the elastic region at radial positions very close to the roots of the notch. On plane B-B, the finite element results agree well with the theoretical solution assuming reduced wall thickness conditions. The deviation from theory is about the same through the entire wall thickness, and the agreement in the elastic region is much better for the short notch case through the deep notch case, 60% overstrain case and also virtually no stress concentration factor $K_{notch}$.

## DISCUSSION

All of the finite element results conclusively show that introducing OD notches in thick-walled cylinders significantly disrupts the stress distribution in the cylinder under any applied loading, particularly in the vicinity of the root radius of the notch. The effect is smaller for shallow notches than deep notches, but is significant in either case. The internal pressure solutions show that the greatest tensile principal stress occurs at the root of the notch in the deep notch case indicating that should such a cylinder be subjected to fatigue, crack initiation would most probably occur at the OD rather than the ID, as in smooth cylinders. For the shallow notch case, the maximum tensile principal stress at the ID and at the root radius of the notch are approximately the same, making crack initiation equally likely at either location.

Recent studies on OD initiated fracture in thick cylinders show that the stress intensity factor increases much more rapidly as the crack grows through the wall thickness of cylinders when cracks initiate at the OD than when cracks initiate at the ID for nonautofrettaged cylinders with pressure loading,[5] and also for autofrettaged cylinders under no external loads.[4] This results in smaller critical crack sizes for OD cracks and enhances the possibility of an unexpected brittle type fracture. Often cylinders can tolerate part-

[4] Kapp, J. A., Unpublished results.

[5] Kapp, J. A. and Eisenstadt, R., Fracture Mechanics, ASTM STP677, C. W. Smith, Ed., American Society for Testing and Materials, 1979, pp. 746-756.

through ID cracks (penny shaped, or semi-elliptical) that penetrate the entire wall thickness before the onset of unstable crack growth. This "leak before break" condition has not been observed in OD initiated failures.

The autofrettage simulation results are alarming, since in all cases the tensile stress occurring in the outer portions of the cylinder are substantially increased when the notches are introduced, further enhancing the likelihood of fatigue initiation at the OD, by increasing the stress ratio ($\sigma_{min}/\sigma_{max}$), which is an important factor in crack initiation.

An equally important, but unexpected result of the autofrettage simulation solutions is the reduction in the value of residual stress which occurs far removed from the notch. In essence, the introduction of the notches relieve some of the residual stresses throughout the entire cylinder. This finding has implications that effect not only the fatigue response of the cylinder, but the static strength of the cylinder as well. The decrease in the maximum compressive stress at the ID also increases the stress ratio applied to this portion of material under fatigue conditions. Also, the smaller compressive residual stresses can be more easily overcome by tensile hoop stresses when the notched cylinder is subjected to internal pressure. Therefore, less pressure is required to initiate yielding in the notched cylinder.

The calculation of the reyielding pressure in real cylinders is complicated by material behavior, such as reversed yielding after the removal of the autofrettage pressure caused by the Bauschinger effect, and the increase in tensile yield strength which often accompanies the cold working of

materials. A first approximation can be made by assuming these effects to be negligible. Assuming the Tresca criterion applies, yielding occurs when:

$$\sigma_0 = \sigma_1 - \sigma_3 \tag{13}$$

In this case the difference in principal stresses is maximum at the ID and $\sigma_1$ is the total hoop stress; the sum of the Lame hoop stress and the hoop residual stress, and $\sigma_3$ is the pressure which is compressive. Using equation (11) with r = a, equation (13) can be rewritten as:

$$\sigma_0 = \frac{\left[1 + \frac{b^2}{a^2}\right]}{\left[\frac{b^2}{a^2} - 1\right]} P + \sigma_{\theta A}(r=a) + P \tag{14}$$

By rearranging equation (14) the pressure required for yielding, the elastic strength pressure, ESP is

$$ESP = \frac{b^2-a^2}{2b^2} \left(\sigma_0 - \sigma_{\theta A}(r=a)\right) \tag{15}$$

To get a good estimate of the elastic strength pressure for the notched cylinder, it is necessary to extrapolate the finite element solutions to the inside radius. This is accomplished easily when it is realized that the residual stresses acting on plane A-A are reduced uniformly with respect to the full thickness theoretical solution. The relieved stresses can be represented accurately bu multiplying the theoretical solution by a factor $R_f$

$$\sigma_{\theta A \text{relieved}} = R_f \sigma_{\theta A}$$

Numerical values for $R_f$ for the cases analyzed are presented in Table I.

For the case of 100% overstrain in a smooth cylinder, the theoretical value of compressive residual stress at the ID is $-.753\ \sigma_0$. From Table I, R for the deep notch 100% overstrain condition is .72, thus the relieved hoop residual stress at r = a is then $-.542\ \sigma_0$. Using these values in equation (15), the elastic strength pressures for a smooth cylinder and a deeply notched cylinder are respectively

$$ESP = 1.753\ \sigma_o\ \left(\frac{b^2-a^2}{2b^2}\right)$$

$$ESP = 1.542\ \sigma_o\ \left(\frac{b^2-a^2}{2b^2}\right)$$

The 12% decrease is significant since often some thick cylinder pressure vessels are designed with little more than 20% safety factor.

## CONCLUSIONS

Autofrettage residual stresses resulting from plastic deformation of a cylinder can be modeled exactly by application of a specific temperature gradient. This method of analysis was used to determine the effect of introducing OD notches on the autofrettage residual stress distributions. The stresses in a notched cylinder subject to internal pressure loading were also determined. The results show that in either of the two notch depths tested, the maximum tensile principal stress occurs at the OD of the cylinder. Also by introducing the notches the autofrettage stresses are relieved to an extent which reduces the pressure required to reyield the cylinder significantly.

REFERENCES


1. Davidson, T. E. and Kendall, D. P., "The Design of High Pressure Containers and Associated Equipment," The Mechanical Behavior of Materials Under Pressure, Pugh, H.L.I.D., Ed., Elsevier Publishing, Amsterdam, 1970.
2. Davidson, T. E., Barton, C. S., Reiner, A. N., and Kendall, D. P., "Overstrain of High-Strength Open-End Cylinders of Intermediate Diameter Ratio," Proceedings of the First International Congress on Experimental Mechanics, Pergamon Press, Oxford, 1963.
3. Davidson, T. E., Eisenstadt, R., and Reiner, A. N., Journal of Basic Engineering, December 1963, pp. 555-565.
4. Kapp, J. A., Unpublished results.
5. Kapp, J. A. and Eisenstadt, R., Fracture Mechanics, ASTM STP 677, C. W. Smith, Ed., American Society for Testing and Materials, 1979, pp. 746-756.
6. Harvey, J. F., Theory and Design of Modern Pressure Vessels, 2nd Edition, Van Nostrand Reinhold, NY, 1974, pp. 61-67.
7. Davidson, T. E., Kendall, D. P., and Reiner, A. N., "Residual Stresses in Thick-Walled Cylinders Resulting from Mechanically Induced Overstrain," Experimental Mechanics, 1963, Vol. 3, pp. 253-262.
8. Kendall, D. P., "The Effect of Material Removal on the Strength of Autofrettaged Cylinders," Watervliet Arsenal Technical Report AD701049, Watervliet, NY, January 1970.
9. Hussain, M. A. and Pu, S. L., "Preliminary Study of the Effect of a Recoil Keyway on the Fatigue Life of the M185 Cannon Tubes," Technical Report ARLCB-TR-78017, Watervliet Arsenal, Watervliet, NY, November 1978.

10. Hussain, M. A., Pu, S. L., Vasilakis, J. D., and O'Hara, P., "Simulation of Partial Autofrettage by Thermal Loads," Submitted to Journal of Pressure Vessels Technology.

11. Timoshenko, S. P. and Goodier, J. N., Theory of Elasticity, 3rd Edition, McGraw-Hill, NY, 1970, p. 448.

12. Kapp, J. A., "The Effect of Autofrettage on Fatigue Crack Propagation in Externally Flawed Thick-Walled Disks," Masters Thesis, Union College, Schenectady, NY, 1976.

TABLE I. STRESS CONCENTRATION FACTORS ($K_{root}$ AND $K_{notch}$) AND STRESS REDUCTION VALUES ($R_f$)

| Loading Condition | Deep Notch $K_{root}$ | Deep Notch $K_{notch}$ | Deep Notch $R_f$ | Shallow Notch $K_{root}$ | Shallow Notch $K_{notch}$ | Shallow Notch $R_f$ |
|---|---|---|---|---|---|---|
| Internal Pressure | 5.4 | 1.6 | 1 | 3.5 | 1.3 | 1 |
| 60% Overstrain | 5.8 | 1.2 | .71 | 3.5 | 1.00 | .72 |
| 100% Overstrain | 6.6 | 1.3 | .70 | 3.7 | 1.02 | .70 |

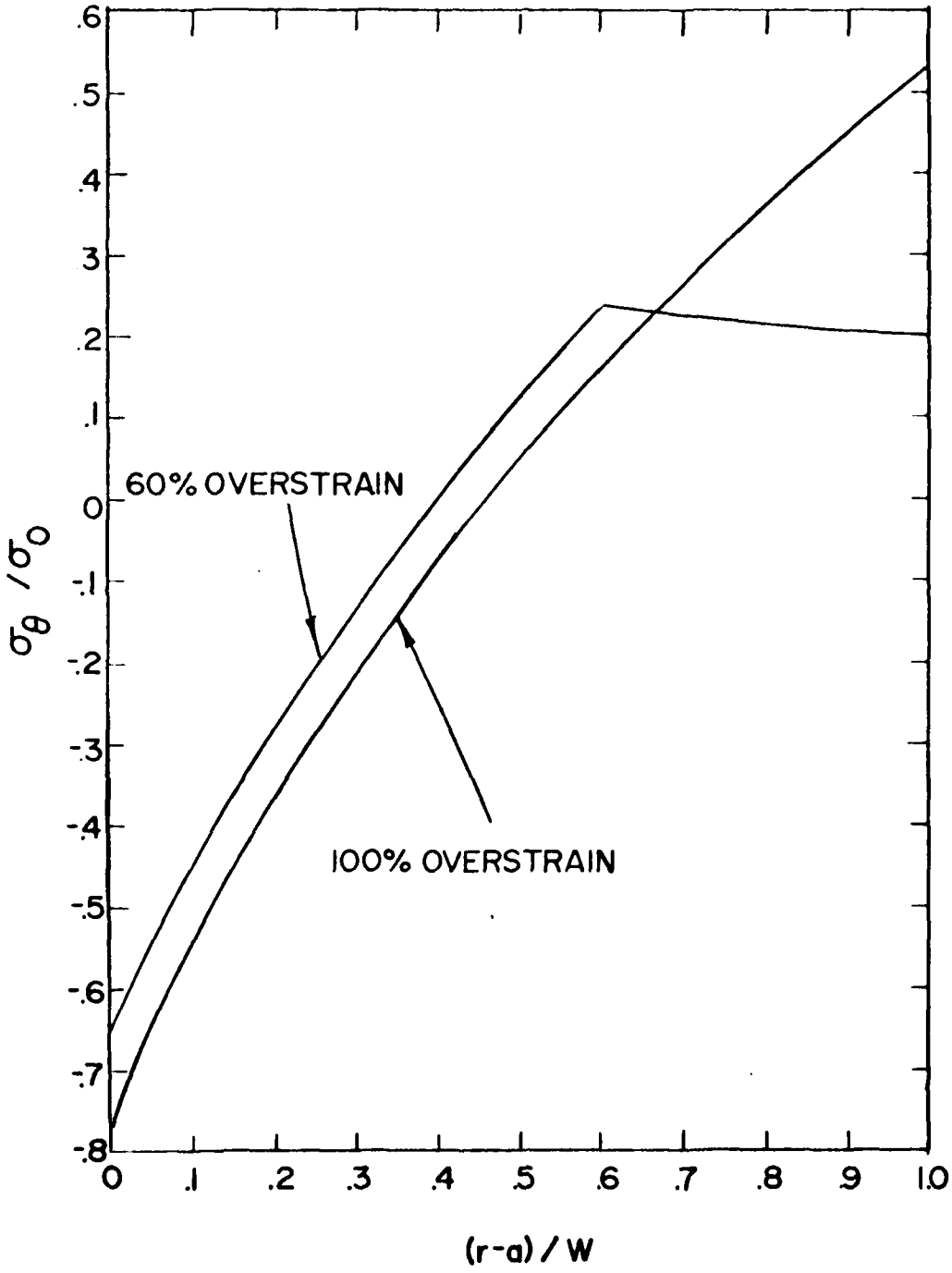


Figure 1. Theoretical autofrettage hoop residual stresses for a thick-walled cylinder of diameter ratio b/a of 1.74.

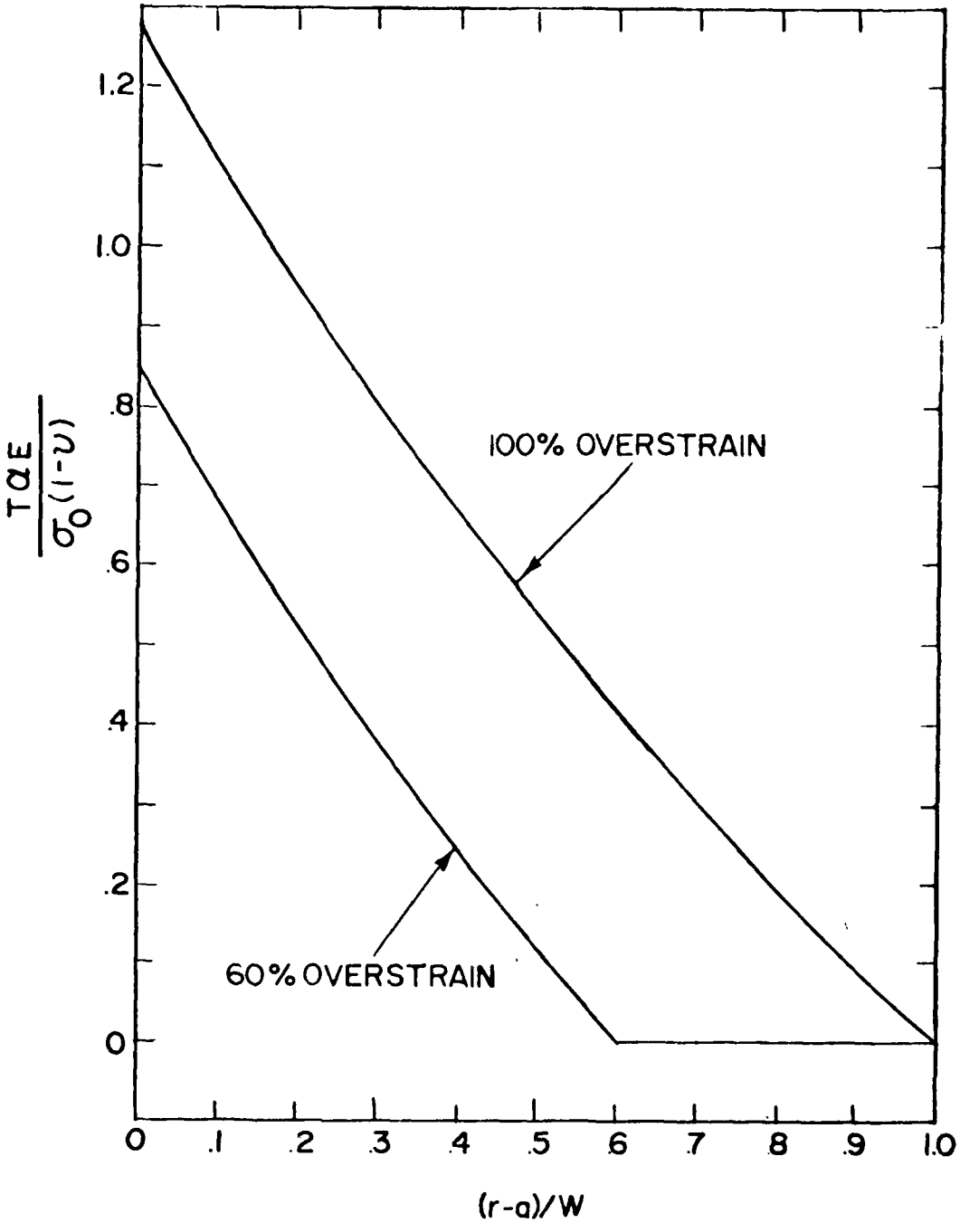


Figure 2. Axisymmetric temperature distributions which produce thermal stress distributions equivalent to the autofrettage stresses in Figure 1.

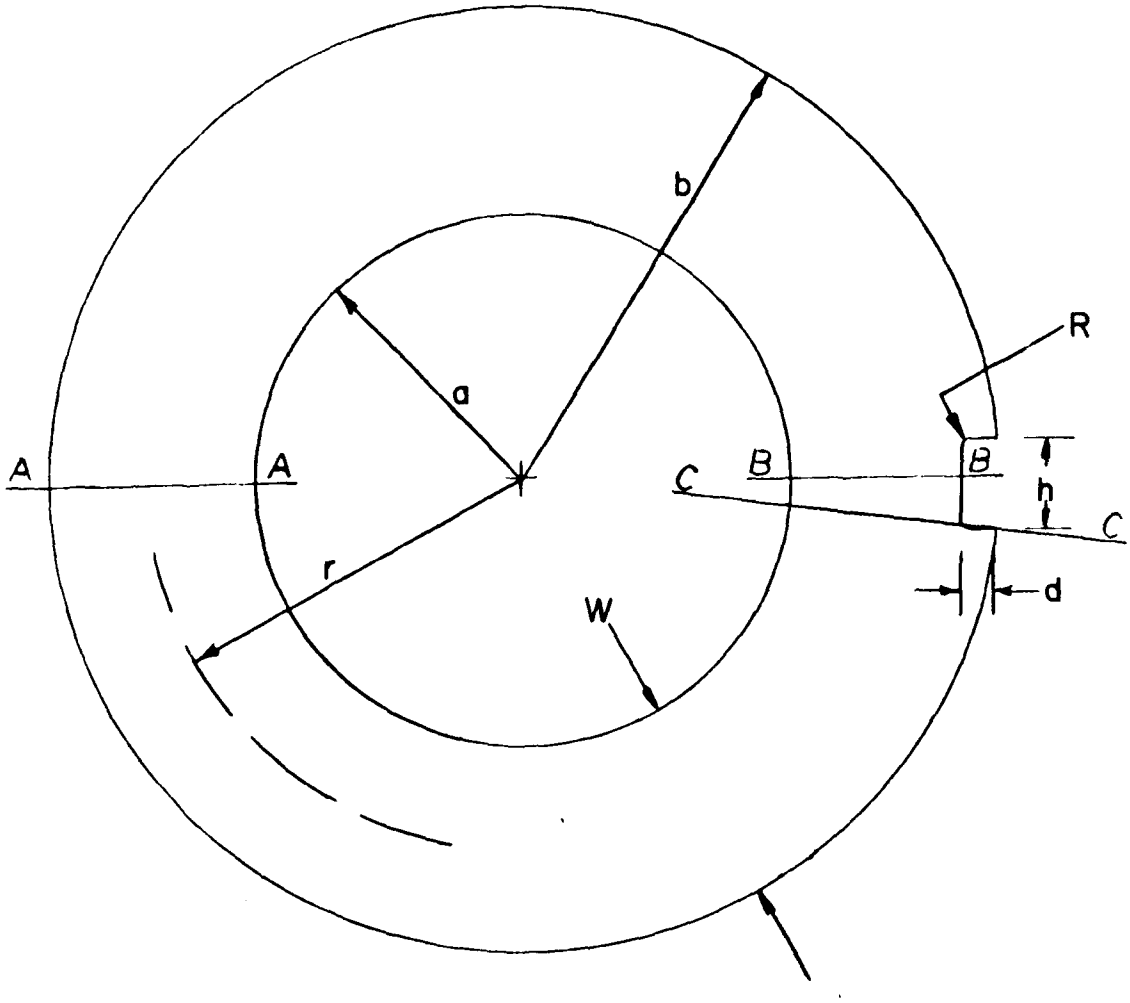


Figure 3. The OD notched cylinder analyzed showing the reference planes where stresses are calculated.

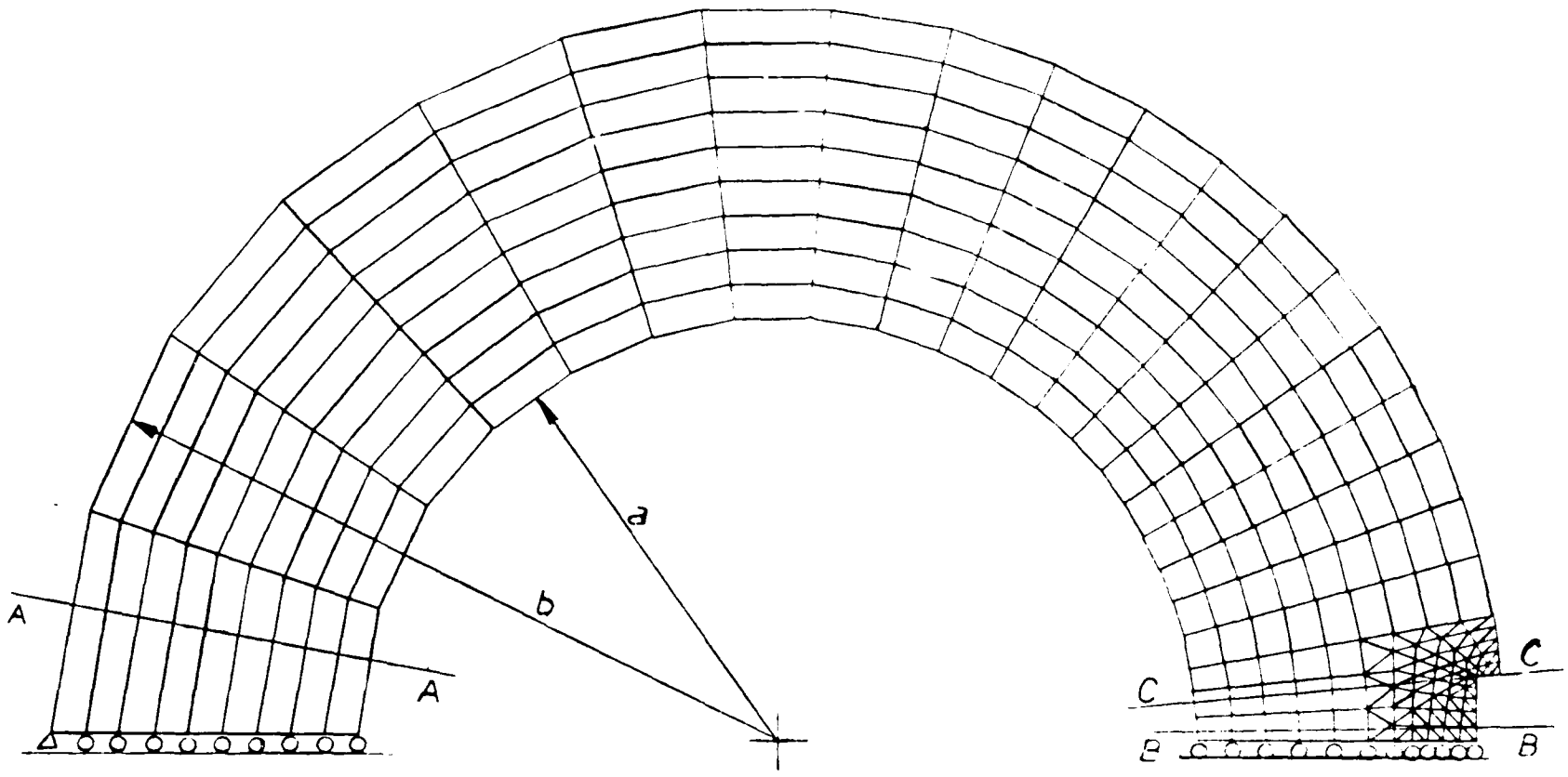


Figure 4. Finite element mesh used to develop the shallow notch solution.

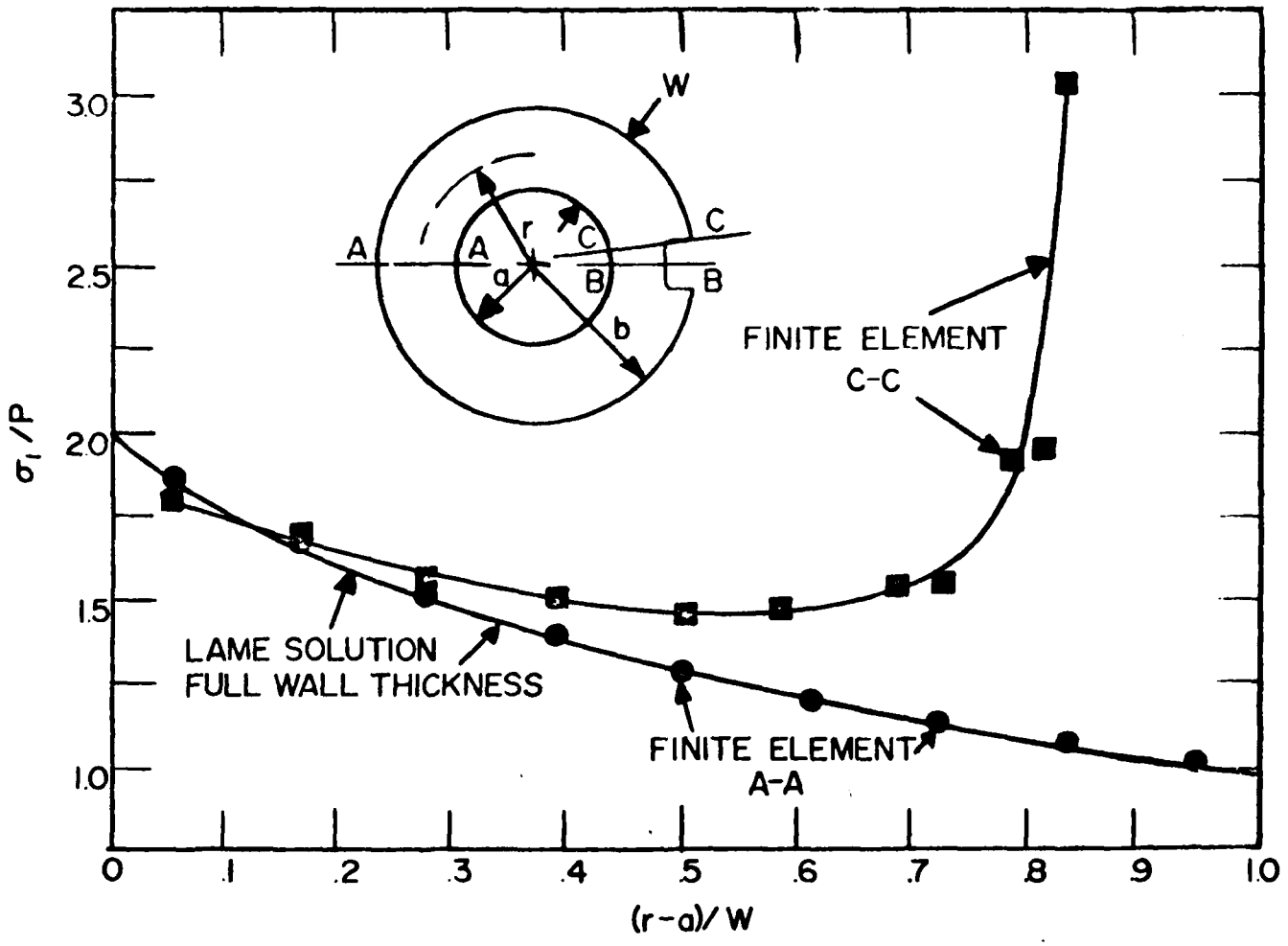


Figure 5. Finite element results for the deep notch internal pressure loading condition.

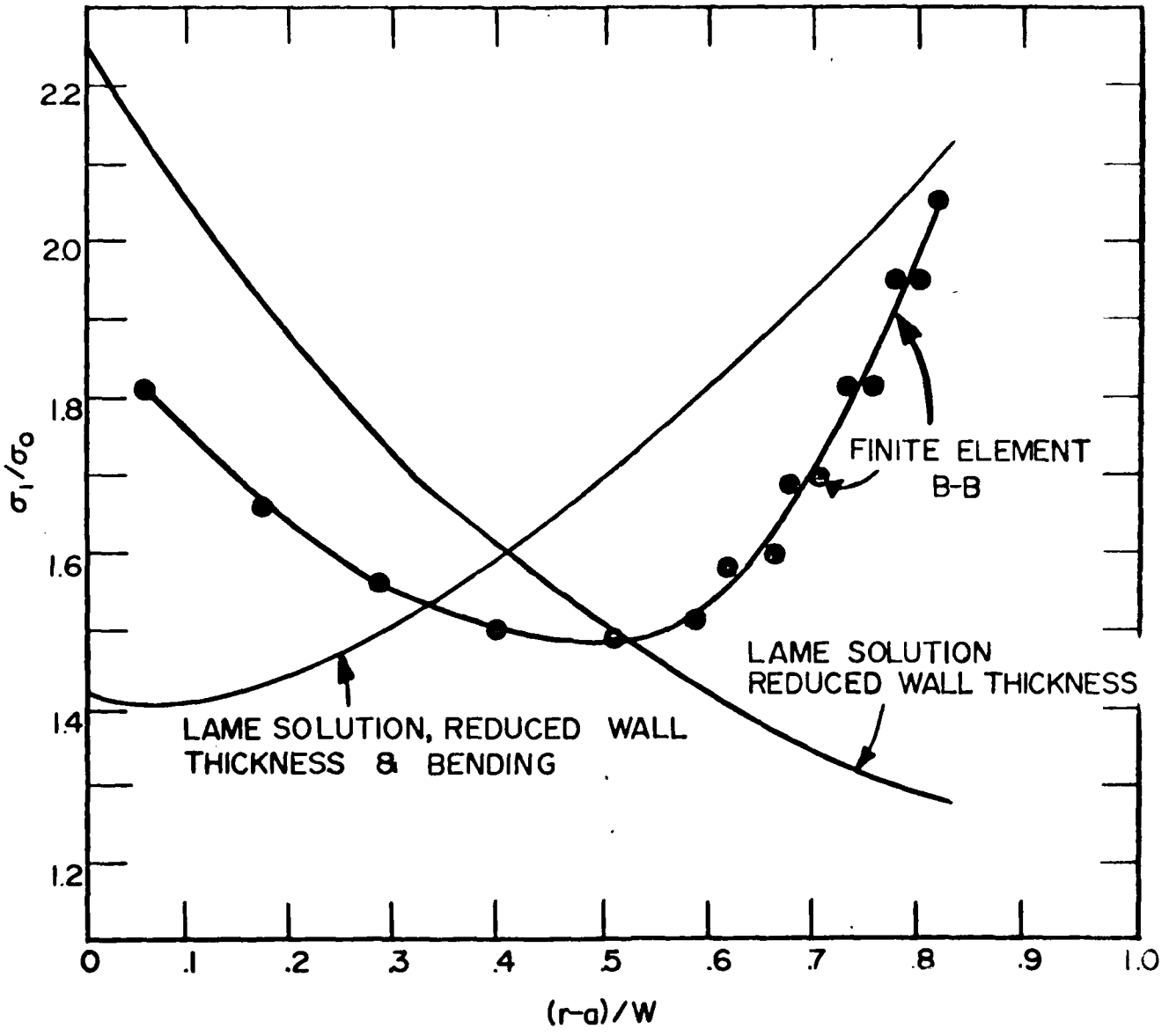


Figure 6. Finite element results for the deep notch internal pressure loading condition.

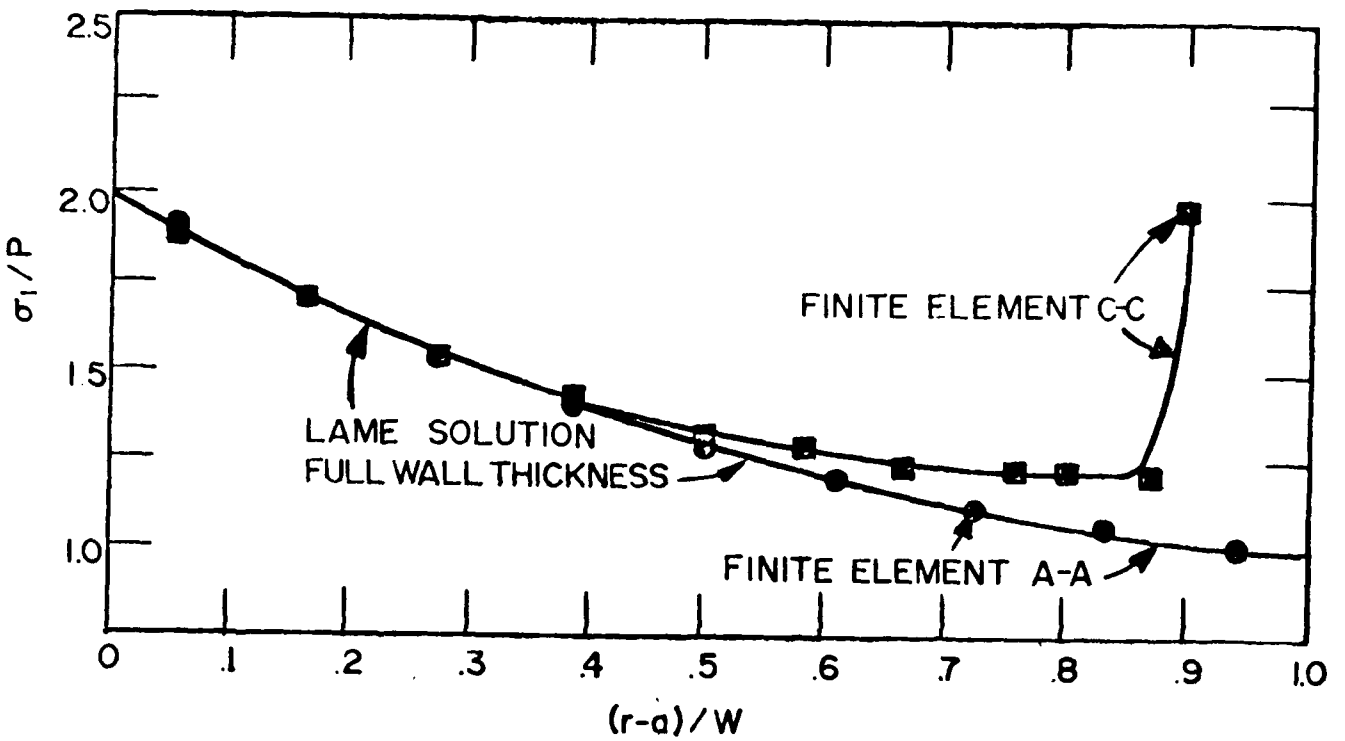


Figure 7. Finite element results for the shallow notch internal pressure loading condition.

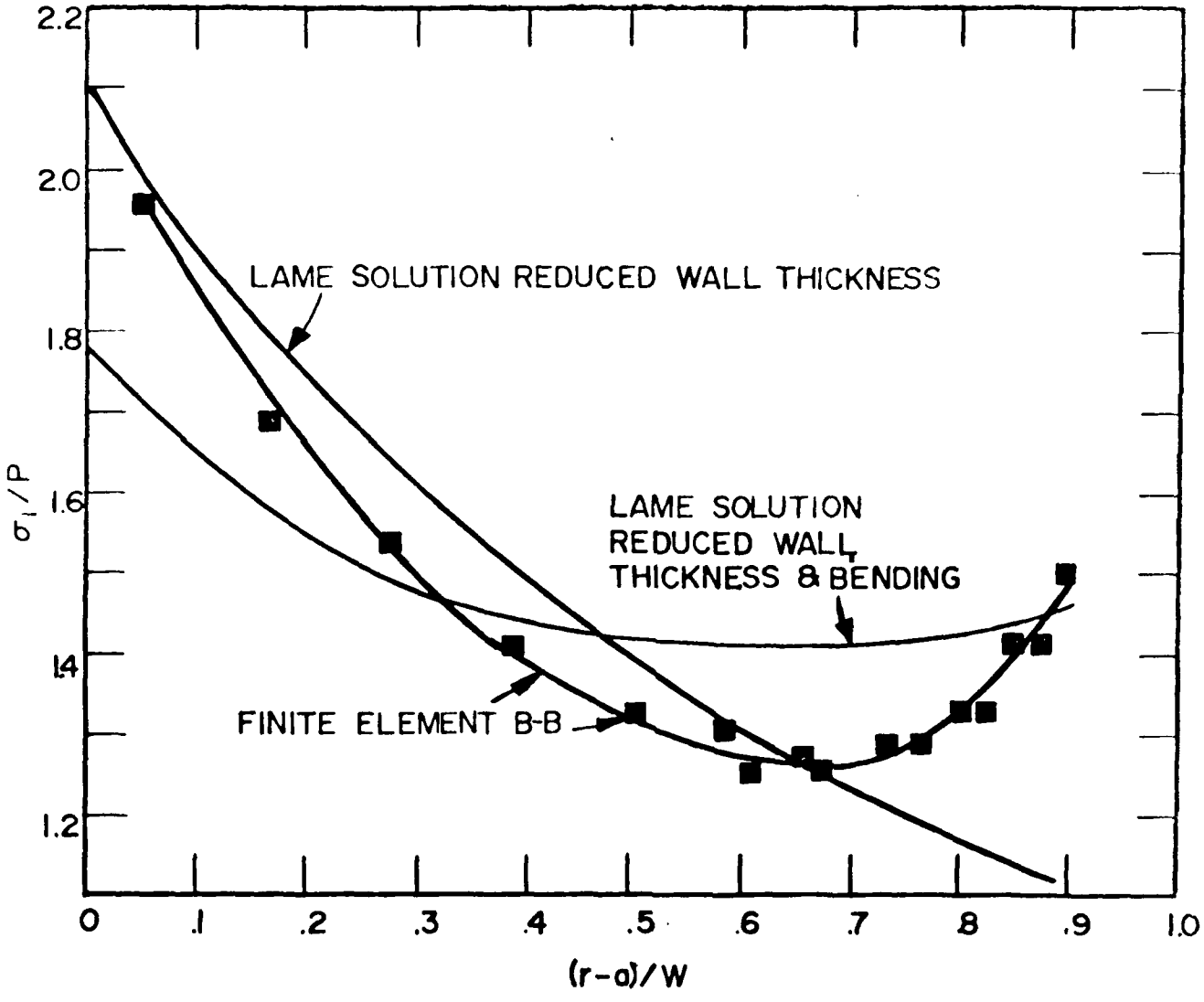


Figure 8. Finite element results for the shallow notch internal pressure loading condition.

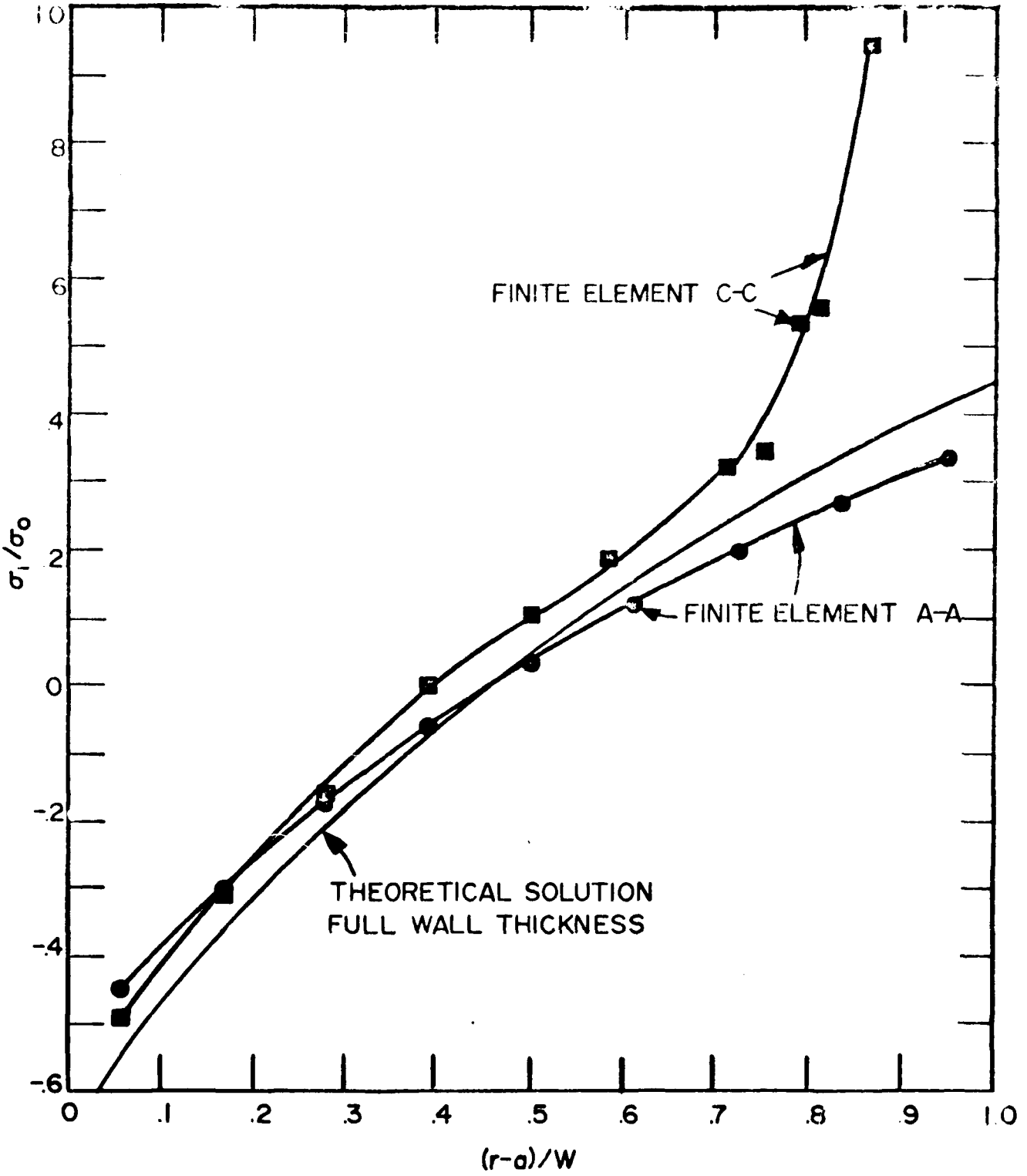


Figure 9. Finite element results for the deep notch 100% overstrain loading condition.

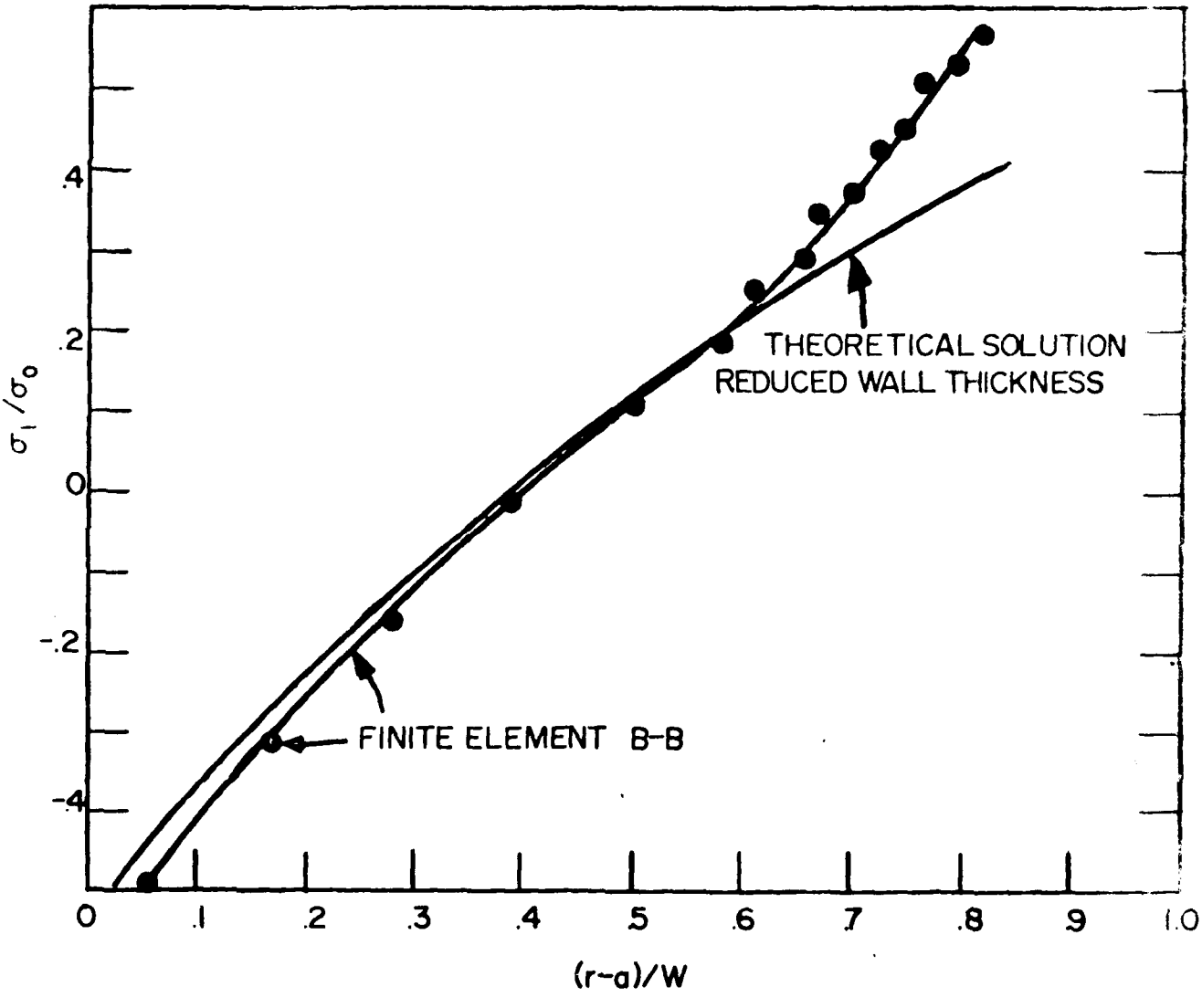


Figure 10. Finite element results for the deep notch 100% overstrain loading condition.

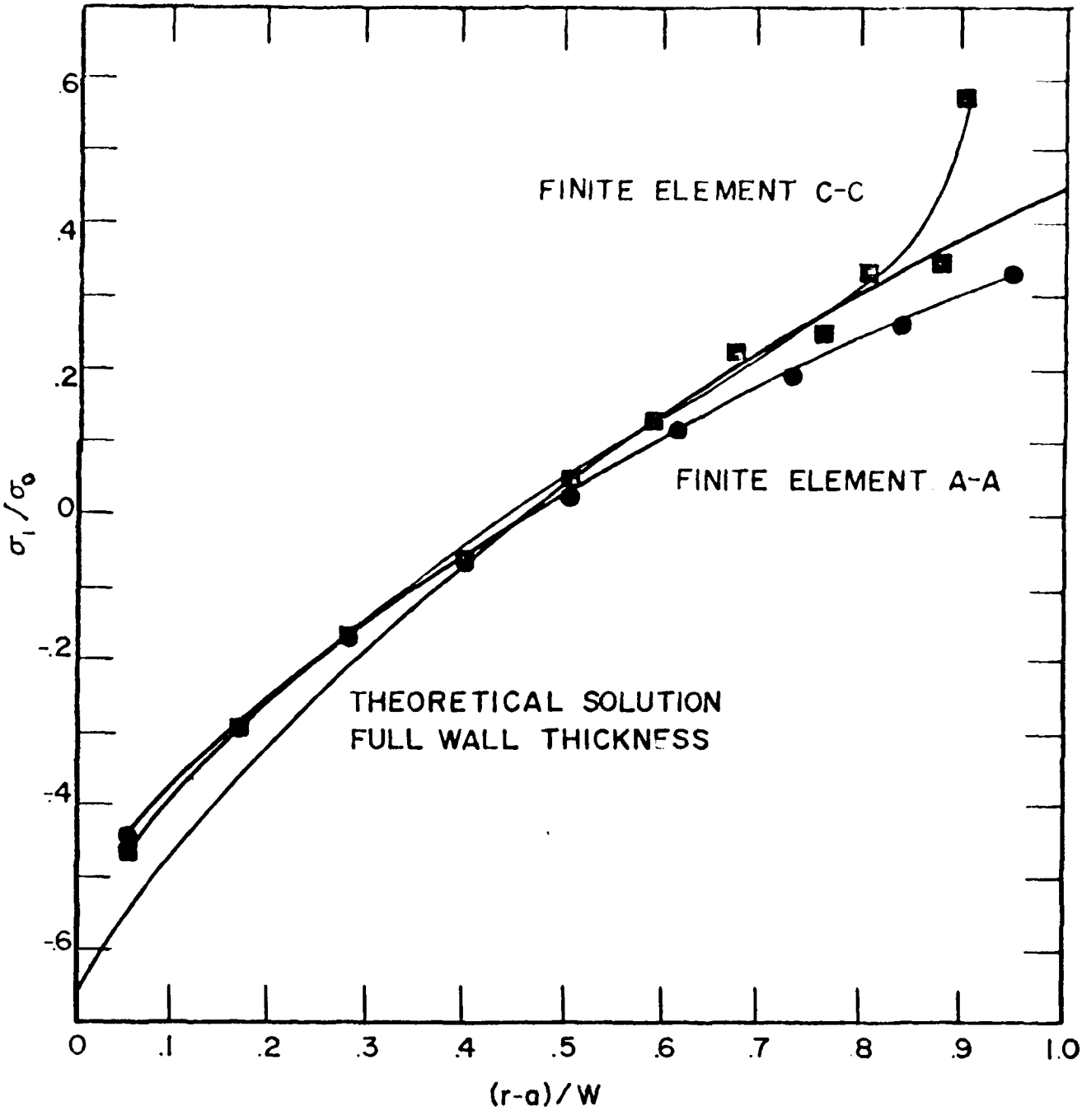


Figure 11. Finite element results for the shallow notch 100% overstrain loading condition.

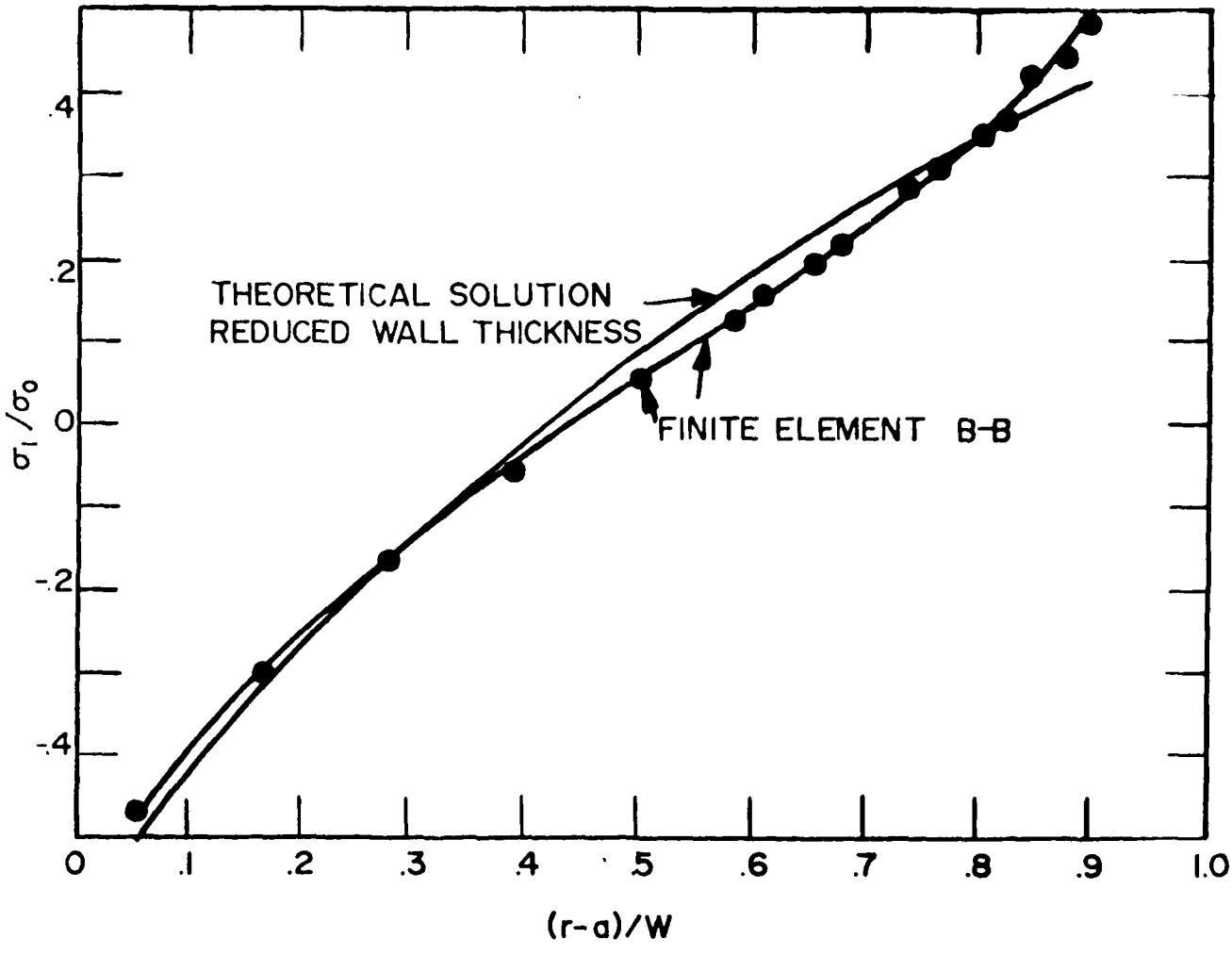


Figure 12. Finite element results for the shallow notch 100% overstrain loading condition.

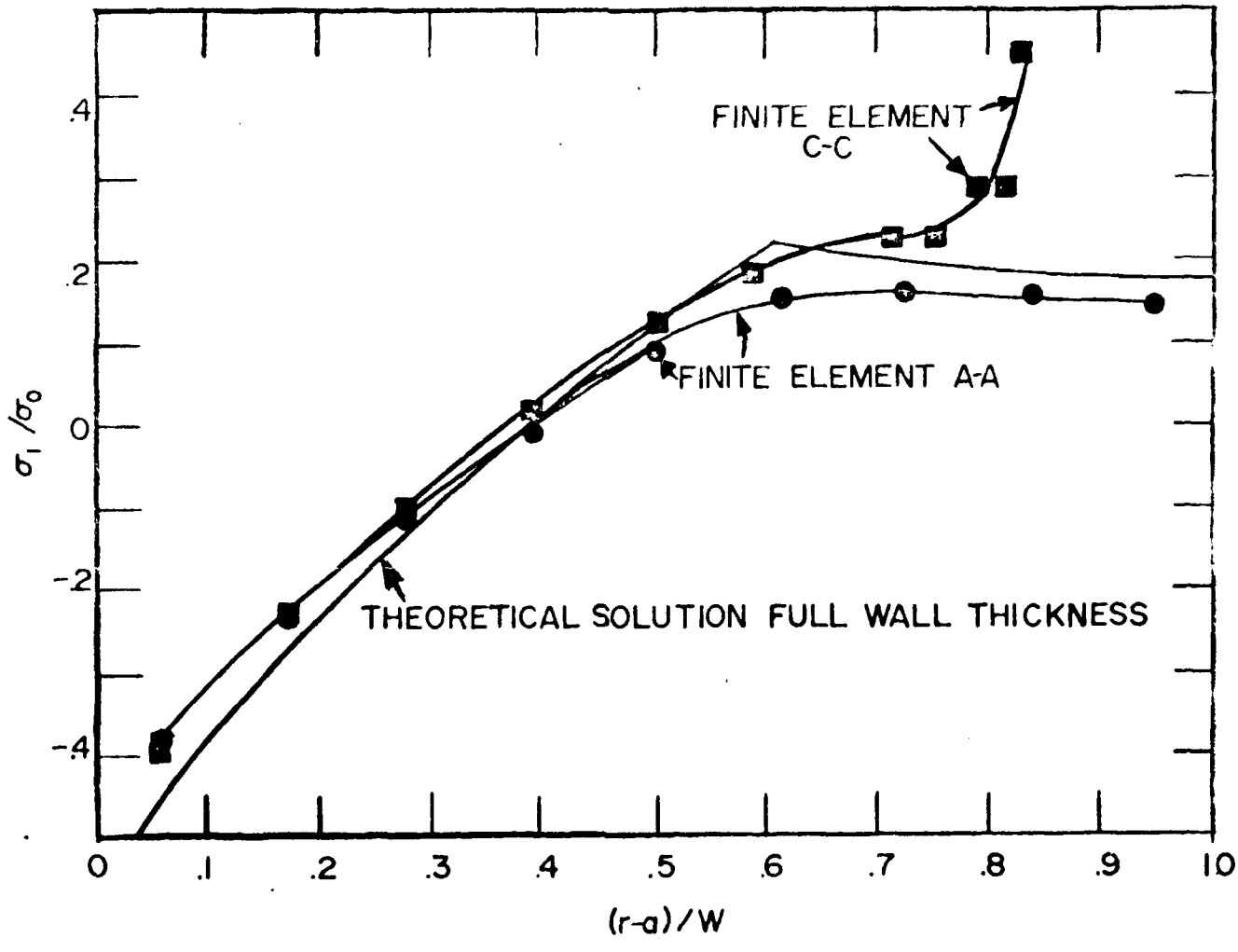


Figure 13. Finite element results for the deep notch 60% overstrain loading condition.

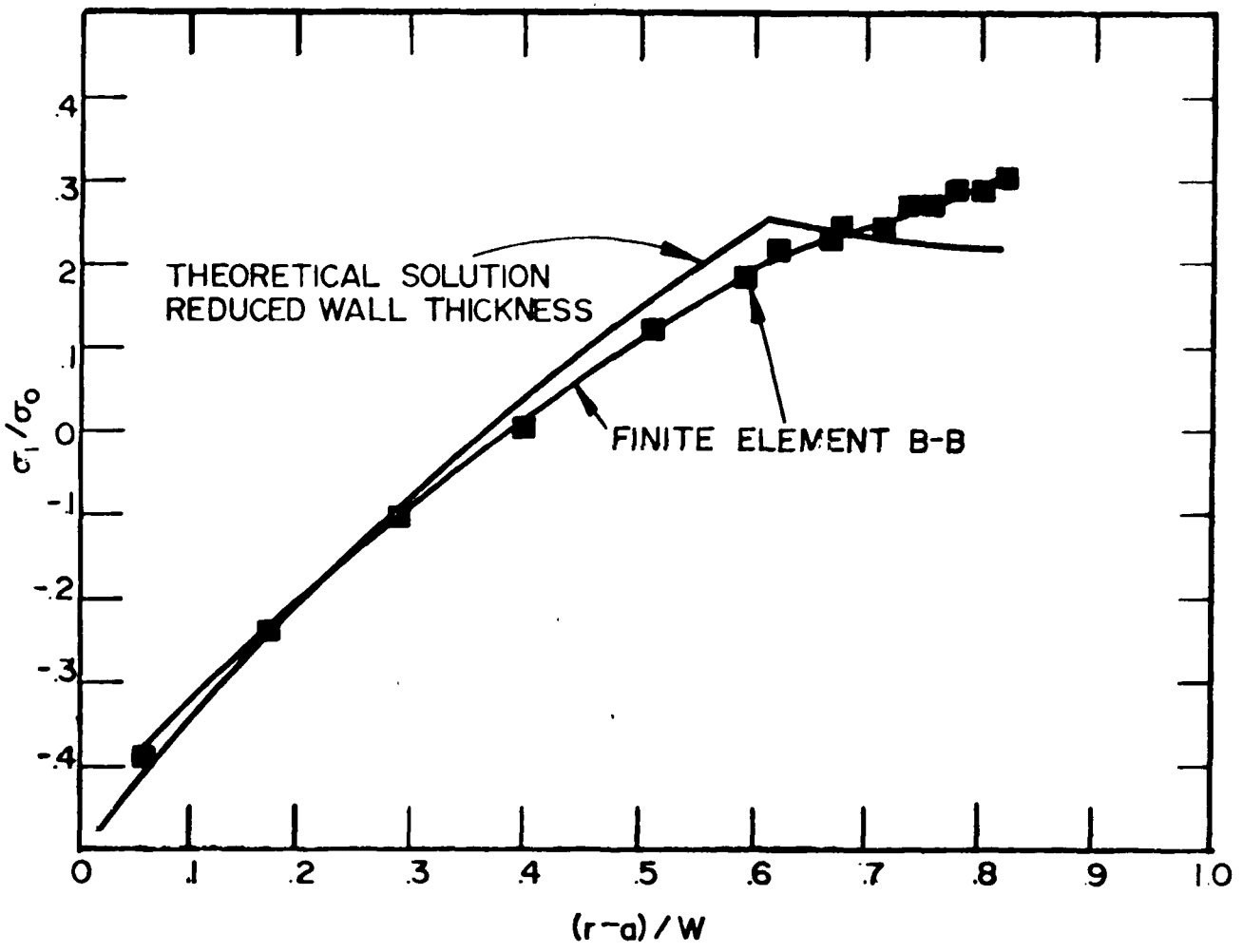


Figure 14. Finite element results for the deep notch 60% overstrain loading condition.

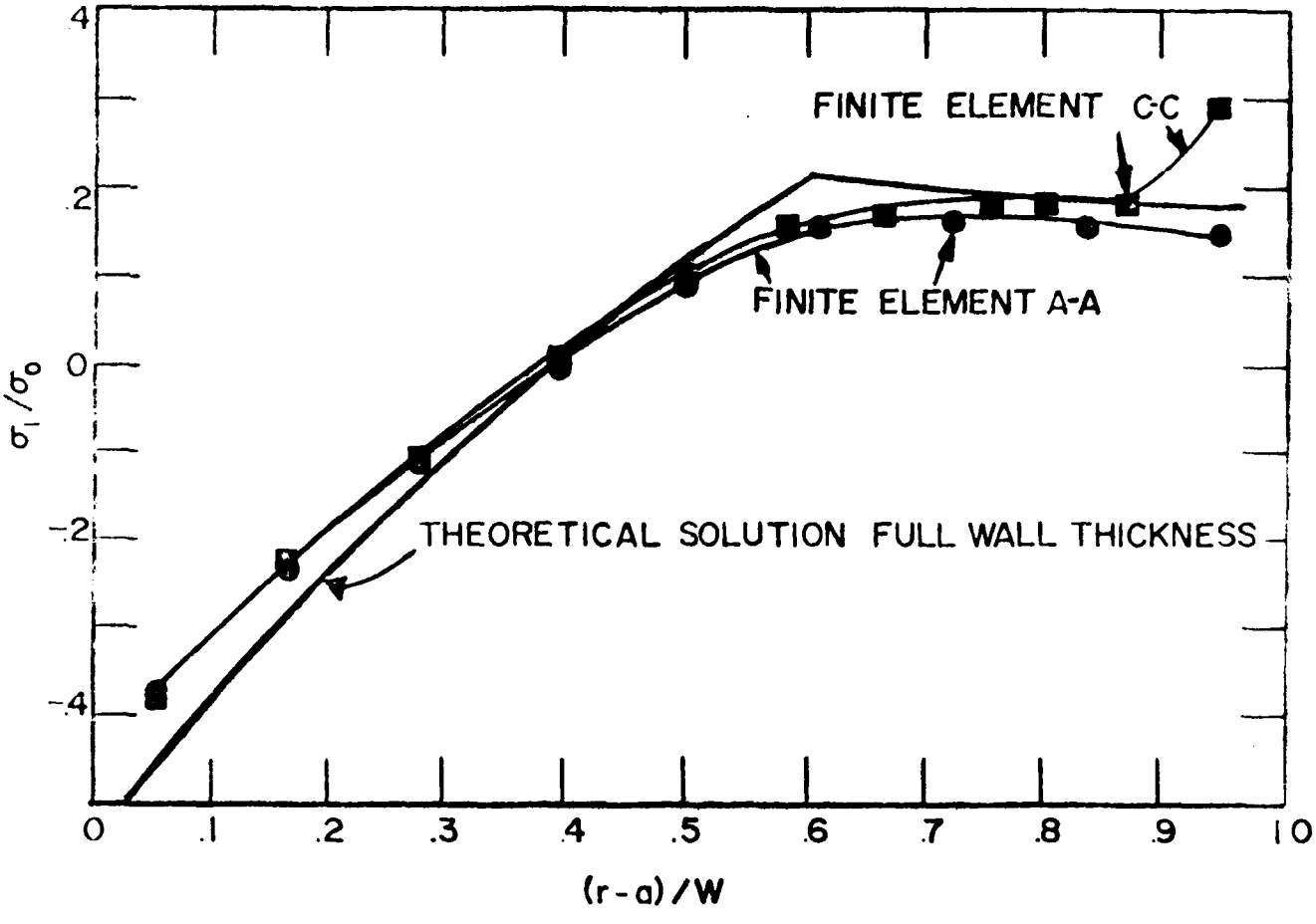


Figure 15. Finite element results for the shallow notch 60% overstrain loading condition.

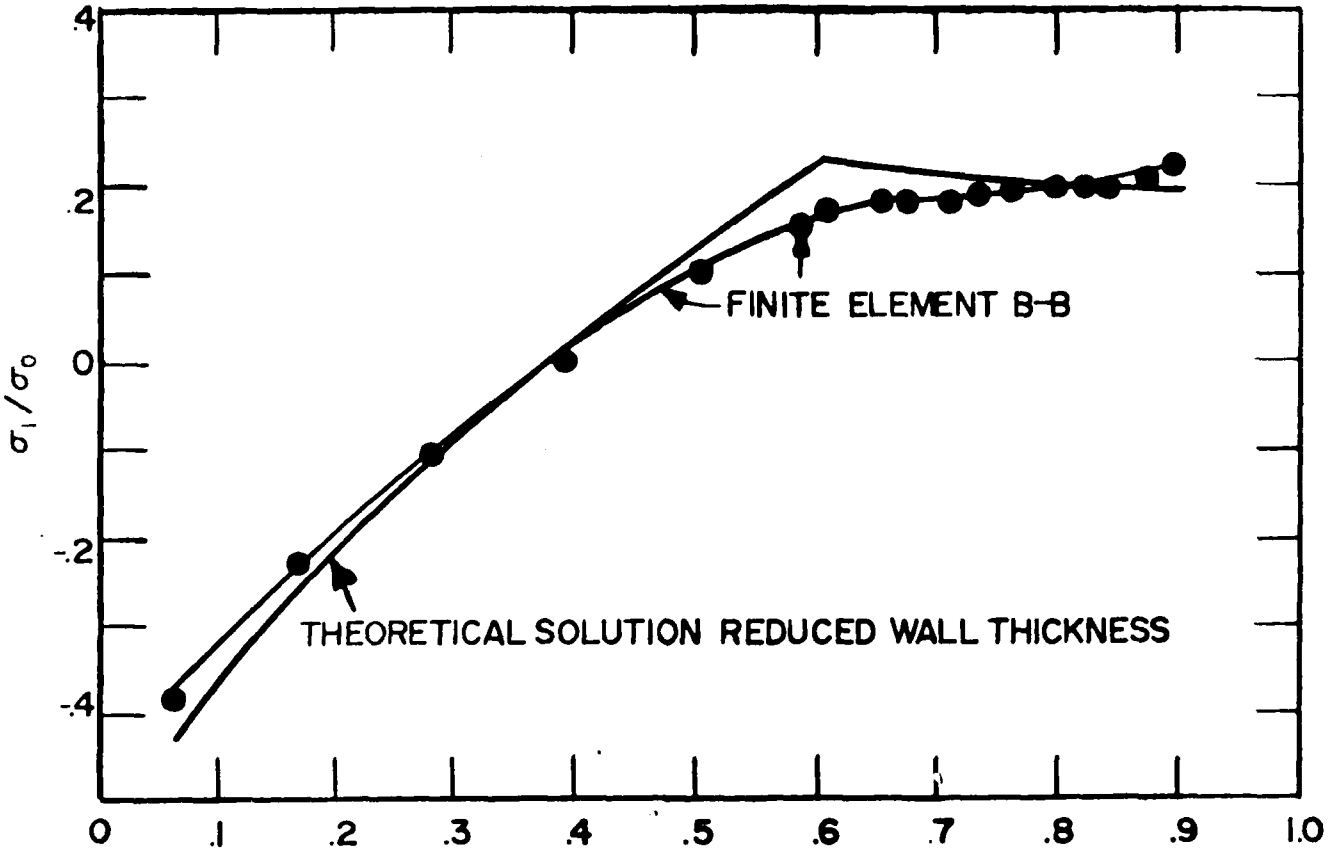


Figure 16. Finite element results for the shallow notch 60% overstrain loading condition.

TECHNICAL REPORT INTERNAL DISTRIBUTION LIST

| | NO. OF COPIES |
|---|---|
| COMMANDER | 1 |
| CHIEF, DEVELOPMENT ENGINEERING BRANCH | 1 |
| ATTN: DRDAR-LCB-DA | 1 |
| -DM | 1 |
| -DP | 1 |
| -DR | 1 |
| -DS | 1 |
| -DC | 1 |
| CHIEF, ENGINEERING SUPPORT BRANCH | 1 |
| ATTN: DRDAR-LCB-SE | 1 |
| -SA | 1 |
| CHIEF, RESEARCH BRANCH | 2 |
| ATTN: DRDAR-LCB-RA | 1 |
| -RC | 1 |
| -RM | 1 |
| -RP | 1 |
| CHIEF, LWC MORTAR SYS. OFC. | 1 |
| ATTN: DRDAR-LCB-M | 1 |
| CHIEF, IMP. 81MM MORTAR OFC. | 1 |
| ATTN: DRDAR-LCB-I | 1 |
| TECHNICAL LIBRARY | 5 |
| ATTN: DRDAR-LCB-TL | |
| TECHNICAL PUBLICATIONS & EDITING UNIT | 2 |
| ATTN: DRDAR-LCB-TL | |
| DIRECTOR, OPERATIONS DIRECTORATE | 1 |
| DIRECTOR, PROCUREMENT DIRECTORATE | 1 |
| DIRECTOR, PRODUCE ASSURANCE DIRECTORATE | 1 |

NOTE: PLEASE NOTIFY ASSOC. DIRECTOR, BENET WEAPONS LABORATORY, ATTN: DRDAR-LCB-TL, OF ANY REQUIRED CHANGES.

TECHNICAL REPORT EXTERNAL DISTRIBUTION LIST

| | NO. OF COPIES |
|---|---|
| ASST SEC OF THE ARMY<br>RESEARCH & DEVELOPMENT<br>ATTN: DEP FOR SCI & TECH<br>THE PENTAGON<br>WASHINGTON, D.C. 20310 | 1 |
| COMMANDER<br>US ARMY MAT DEV & READ. COMD<br>ATTN: DRCDE<br>5001 EISENHOWER AVE<br>ALEXANDRIA, VA 22333 | 1 |
| COMMANDER<br>US ARMY ARRADCOM<br>ATTN: DRDAR-LC | 1 |
| -LCA (PLASTICS TECH EVAL CEN) | 1 |
| -LCE | 1 |
| -LCM | 1 |
| -LCS | 1 |
| -LCW | 1 |
| -TSS(STINFO)<br>DOVER, NJ 07801 | 2 |
| COMMANDER<br>US ARMY ARRCOM<br>ATTN: DRSAR-LEP-L<br>ROCK ISLAND ARSENAL<br>ROCK ISLAND, IL 61299 | 1 |
| DIRECTOR<br>US Army Ballistic Research Laboratory<br>ATTN: DRDAR-TSB-S (STINFO)<br>ABERDEEN PROVING GROUND, MD 21005 | 1 |
| COMMANDER<br>US ARMY ELECTRONICS COMD<br>ATTN: TECH LIB<br>FT MONMOUTH, NJ 07703 | 1 |
| COMMANDER<br>US ARMY MOBILITY EQUIP R&D COMD<br>ATTN: TECH LIB<br>FT BELVOIR, VA 22060 | 1 |

| | NO. OF COPIES |
|---|---|
| COMMANDER<br>US ARMY TANK-AUTMV R&D COMD<br>ATTN: TECH LIB - DRDTA-UL | 1 |
| MAT LAB - DRDTA-RK<br>WARREN MICHIGAN 48090 | 1 |
| COMMANDER<br>US MILITARY ACADEMY<br>ATTN: CHMN, MECH ENGR DEPT<br>WEST POINT, NY 10996 | 1 |
| COMMANDER<br>REDSTONE ARSENAL<br>ATTN: DRSMI-RR | 2 |
| -RRS | 1 |
| -RSM<br>ALABAMA 35809 | 1 |
| COMMANDER<br>ROCK ISLAND ARSENAL<br>ATTN: SARRI-ENM (MAT SCI DIV)<br>ROCK ISLAND, IL 61202 | 1 |
| COMMANDER<br>HQ, US ARMY AVN SCH<br>ATTN: OFC OF THE LIBRARIAN<br>FT RUCKER, ALABAMA 36362 | 1 |
| COMMANDER<br>US ARMY FGN SCIENCE & TECH CEN<br>ATTN: DRXST-SD<br>220 7TH STREET, N.E.<br>CHARLOTTESVILLE, VA 22901 | 1 |
| COMMANDER<br>US ARMY MATERIALS & MECHANICS RESEARCH CENTER<br>ATTN: TECH LIB - DRXMR-PL<br>WATERTOWN, MASS 02172 | 2 |

NOTE: PLEASE NOTIFY COMMANDER, ARRADCOM, ATTN: BENET WEAPONS LABORATORY, DRDAR-LCB-TL, WATERVLIET ARSENAL, WATERVLIET, N.Y. 12189, OF ANY REQUIRED CHANGES.

TECHNICAL REPORT EXTERNAL DISTRIBUTION LIST (CONT)

| | NO. OF COPIES |
|---|---|
| COMMANDER<br>US ARMY RESEARCH OFFICE<br>P.O. BOX 12211<br>RESEARCH TRIANGLE PARK, NC 27709 | 1 |
| COMMANDER<br>US ARMY HARRY DIAMOND LAB<br>ATTN: TECH LIB<br>2800 POWDER MILL ROAD<br>ADELPHIA, MD 20783 | 1 |
| DIRECTOR<br>US ARMY INDUSTRIAL BASE ENG ACT<br>ATTN: DRXPE-MT<br>ROCK ISLAND, IL 61201 | 1 |
| CHIEF, MATERIALS BRANCH<br>US ARMY R&S GROUP, EUR<br>BOX 65, FPO N.Y. 09510 | 1 |
| COMMANDER<br>NAVAL SURFACE WEAPONS CEN<br>ATTN: CHIEF, MAT SCIENCE DIV<br>DAHLGREN, VA 22448 | 1 |
| DIRECTOR<br>US NAVAL RESEARCH LAB<br>ATTN: DIR, MECH DIV<br>CODE 26-27 (DOC LIB)<br>WASHINGTON, D. C. 20375 | 1<br>1 |
| NASA SCIENTIFIC & TECH INFO FAC<br>P. O. BOX 8757, ATTN: ACQ BR<br>BALTIMORE/WASHINGTON INTL AIRPORT<br>MARYLAND 21240 | 1 |

| | NO. OF COPIES |
|---|---|
| COMMANDER<br>DEFENSE TECHNICAL INFO CENTER<br>ATTN: DTIA-TCA<br>CAMERON STATION<br>ALEXANDRIA, VA 22314 | 12 |
| METALS & CERAMICS INFO CEN<br>BATTELLE COLUMBUS LAB<br>505 KING AVE<br>COLUMBUS, OHIO 43201 | 1 |
| MECHANICAL PROPERTIES DATA CTR<br>BATTELLE COLUMBUS LAB<br>505 KING AVE<br>COLUMBUS, OHIO 43201 | 1 |
| MATERIEL SYSTEMS ANALYSIS ACTV<br>ATTN: DRXSY-MP<br>ABERDEEN PROVING GROUND<br>MARYLAND 21005 | 1 |

NOTE: PLEASE NOTIFY COMMANDER, ARRADCOM, ATTN: BENET WEAPONS LABORATORY, DRDAR-LCB-TL, WATERVLIET ARSENAL, WATERVLIET, N.Y. 12189, OF ANY REQUIRED CHANGES.

END

DATE
FILMED

8-80

DTIC